Journal of the Serbian Chemical Society
JSCS-info@shd.org.rs • www.shd.org.rs/JSCS
J. Serb. Chem. Soc. *82* (6) 607–625 (2017)
JSCS–4991
UDC 620.1/.2:66.017:544.112+544.6.076.2–039.34:546.41'185:544.2.004.12
Authors' review

AUTHORS' REVIEW

Molecular designing of nanoparticles and functional materials

NENAD L. IGNJATOVIĆ, SMILJA MARKOVIĆ, DRAGANA JUGOVIĆ and DRAGAN P. USKOKOVIĆ*

Institute of Technical Sciences of the Serbian Academy of Sciences and Arts, Knez Mihailova 35/IV, P. O. Box 377, 11000 Belgrade, Serbia

(Received 7 December, revised 15 December, accepted 23 December 2016)

Abstract: The interdisciplinary research team implemented the program titled "Molecular designing of nanoparticles with controlled morphological and physicochemical characteristics and functional materials based on them" (MODENAFUNA), between 2011 and 2016, gaining new knowledge significant to the further improvement of nanomaterials and nanotechnologies. It gathered under its umbrella six main interrelated topics pertaining to the design and control of morphological and physicochemical properties of nanoparticles and functional material based on them using new methods of synthesis and processing: 1) inorganic nanoparticles, 2) cathode materials for lithium-ion batteries, 3) functional ceramics with improved electrical and optical properties, 4) full density nanostructured calcium phosphate and functionally-graded materials, 5) nano-calcium phosphate in bone tissue engineering and 6) biodegradable micro- and nano-particles for the controlled delivery of medicaments.

Keywords: molecular designing; nanoparticles; functional materials.

CONTENTS

* Corresponding author. E-mail: dragan.uskokovic@itn.sanu.ac.rs
https://doi.org/10.2298/JSC16120700111

1. INTRODUCTION

Project "Molecular designing of nanoparticles with controlled morphological and physicochemical characteristics and functional materials based on them" was funded by the Ministry for Education, Science and Technological Development of Serbia, within its program of integral and interdisciplinary research (III--45004). By molecular designing we mean the process of the mixing of precursor species at the molecular level using one or multiple soft chemistry methods, enabling the formation of particles (or compacts) with predefined geometrical distributions of constituent phases. Various bottom-up and top-down innovative processes of nanoparticle synthesis by molecular processing have for a long time been the main activities within the research program of the group which implemented this project (Fig. 1).

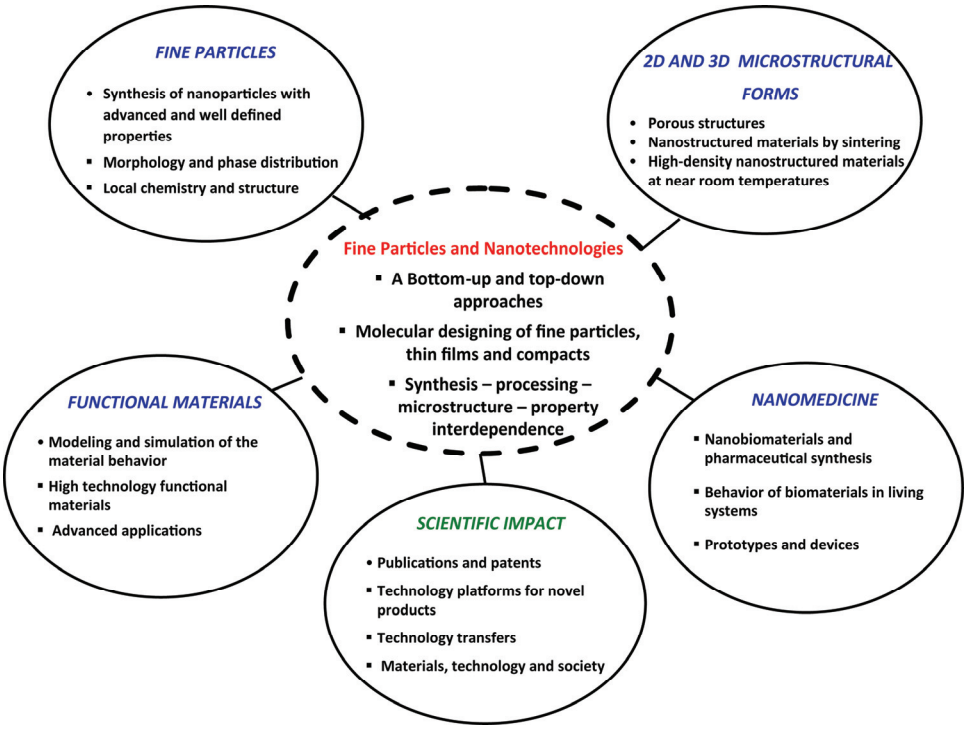

Fig. 1. Global scheme of activities in the field of fine particles and nanotechnology.

A wide range of functional materials, including electronic, electrochemical, optical and catalytic materials, biomaterials and pharmaceutical materials intended as drug-delivery carriers with controlled release of medicaments are the focus of research programs in the field of advanced materials and nano-technologies. The aim of all these activities is to find out solutions to some of the critical problems of sustainable development in the fields of healthcare, environ-

ment, energy, water and other global challenges dominating our present and near future.

The activities of the project were carried out within six main interrelated topics focused on the acquisition of fundamental and applicative knowledge in the molecular design of nanoparticles with a controlled morphology and physico-chemical properties and development of functional materials based on them: 1) inorganic nanoparticles, 2) cathode materials for lithium-ion batteries, 3) functional ceramics with improved electrical and optical properties, 4) full density nano-structured calcium phosphate and functionally graded materials, 5) nano--calcium phosphate in bone tissue engineering and 6) biodegradable micro- and nano-particles for the controlled delivery of medicaments.

2. INORGANIC NANOPARTICLES

The analysis of publications in the field of nanotechnology over the past 15 years shows that nanoparticles have been the most studied topic in the area of nanomaterials, indicating their great scientific and technological potential. Far behind them are nanotubes, nanocrystals and nanocomposites. Nanoparticles also hold the top position in publication quality, as measured by the Hirsch index value for the published articles in the same period. Our research was focused on finding out the new methods for the synthesis and processing of hydroxyapatite (HAp), Fe_2O_3, Au and ZnO nanoparticles with controlled structures, properties and morphology.

Mammalian bone tissues mostly consist of calcium phosphate nanoparticles, specifically HAp. The aim of the application of methods such as sonochemistry,[1] mechanochemistry, sol–gel synthesis, hydrothermal processing,[2] and other[3] in laboratory conditions was to obtain nanoparticles of HAp with a controlled structure and morphology. Numerous factors influence the formation mechanism of HAp particles during precipitation: Ca/P mole ratio, pH, temperature, surface additives, etc. Chemical precipitation method was developed for the synthesis of carbonated hydroxyapatite (CHAp) nano-powder with a potential application as a bone substitute in oral and maxillofacial surgery. The extent to which synthesized CHAp matches the corresponding biological material, extracted from human mandibular bone (BHAp), was investigated by comparing their phase composition, crystal structure and morphology. A good correlation between the unit cell parameters, average crystallite size, morphology, carbonate content and crystallographic positions of carbonate ions in the natural and synthetic HAp samples was found. It was shown that the AB-type CHAp synthesized by the precipitation method simulated the phase composition, crystal structure and morphology of biological apatite from the human mandible bone.[4]

HAp can also be used for a variety of applications, including the controlled delivery and release of therapeutic agents (extracellularly or intracellularly),

magnetic resonance imaging and hyperthermia therapy, cell separation, blood detoxification, peptide or oligonucleotide chromatography and ultrasensitive detection of biomolecules, and *in vivo* and *in vitro* gene transfection.[5] The ultrasonic processing method was applied to design nanoparticulate carriers based on HAp for tuneable and sustained delivery of antibiotics. Such carriers have a potential in the treatment of bone defects caused by serious infections.[1]

A simple and green solvothermal procedure was developed for the synthesis of high-quality monodisperse and spherical magnetic iron oxide particles. Glucose was used as a reducing agent and the procedure did not require a protective atmosphere. By optimizing the process parameters, particles with a uniform size distribution, with the size of 5 nm, were obtained. In this study, we also transformed hydrophobic magnetic nanoparticles into water-soluble particles using poly(L-lactide).[6]

Water-soluble gold nanoparticles were synthesized by a facile solvothermal process using a $HAuCl_4$ (gold(III) chloride solution) and oleylamine mixture. Oleylamine serves as a reduction agent, as well as a stabilizer for nanoparticle surfaces. Particle sizes were adjusted by modulating the reaction temperature and time. The addition of oleylamine to the reaction promoted monodisperse, hydrophobic, and well-characterized small (~7 nm) gold nanoparticles (Fig. 2). The lipid functionalization of the synthesized nanoparticles resulted in water-soluble gold nanoparticles.[7] The hydrophobic heads of lipids bound to the particles, leaving the hydrophilic tails free so that particles became water-soluble and suitable for potential biomedical applications.

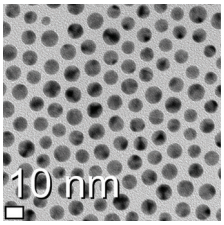

Fig. 2. TEM image of monodisperse and spherical gold nanoparticles.

Mechanochemical processing and successive thermal decomposition were used for the synthesis of zinc oxide (ZnO) nanoparticles.[8] It has been shown that an aqueous solution of oxalic acid has a profound effect on the preparation of ZnO particles, acting both as the starting reactant and the passivating agent in the first-step of the synthesis. We have shown that the dry milling procedure yields ZnO particles with average sizes between 50 and 90 nm, while in the wet-milling procedure the average particle size was reduced to between 15 and 50 nm.[8] We synthesized ZnO particles of different sizes and morphologies with the assistance of different types of surface stabilizing agents – poly(vinyl pyrolidone) (PVP), poly(vinyl alcohol) (PVA) and poly(α,γL-glutamic acid) (PGA) – *via* a low-tem-

perature hydrothermal procedure. ZnO particles of various forms and dimensions showed very good antibacterial effect against gram-positive and gram-negative bacteria during *in vitro* tests. The highest microbial cell reduction rate was recorded for the synthesized ZnO powder consisting of nanospherical particles.[9]

3. CATHODE MATERIALS FOR LITHIUM ION BATTERIES

A simple and low-cost synthesis route was applied for the preparation of a composite powder consisting of the olivine type $LiFePO_4$ and carbon. The precursor powder was prepared by aqueous precipitation in molten stearic acid and a subsequent heat treatment in inert atmosphere at different temperatures (600, 700 and 800 °C).[10] Stearic acid served both as a surfactant and a dispersant throughout the precursor formation, but also as a carbon source. Namely, during the pyrolytic degradation in inert atmosphere, stearic acid decomposed to carbon, creating reductive volatiles that prevent the oxidation of Fe^{2+}. The obtained powders were composites of olivine type $LiFePO_4$ and carbon, with the presence of heterosite $FePO_4$ as a minor phase. The electrochemical performance was investigated trough galvanostatic charge/discharge tests. The powder heated at 700 °C had the best electrochemical performance: it delivered a capacity of 160 mA h g^{-1}, *i.e.*, 94 % of the theoretical capacity. The applied synthesis route can be easily scaled up for commercialization, since it requires neither specific nor expensive equipment.

The same approach was applied for the synthesis of fluorine-doped $LiFePO_4$/C (Fig. 3). This time, LiF was used both as lithium and fluorine source, and the temperature of 700 °C was chosen as an annealing temperature[11]. Although fluorine ions were present in excess, the doping with fluorine was attainable only for a small fluorine content (2 at. %). The prepared powder exhibited an excellent high-rate performance. X-ray powder diffraction confirmed that fluorine doping preserved the olivine structure. A careful crystal structure refinement revealed that fluorine ions occupied only the O(2) oxygen site. Theoretical modelling confirmed the experimental finding that the O(2) site was also energetically the most stable solution. Particularly interesting is the predicted formation of a metallic solution with a finite density of states at the Fermi energy for the fluorine-doped sample.[11] In our research, we also examined influence of fluorine doping on the structural and electrical properties of the $LiFePO_4$ the carbon-free powder. A small amount of incorporated fluorine enhances the electrical conductivity from 4.6×10^{-7} to 2.3×10^{-6} S cm^{-1}.[12]

Another time- and energy- saving method was also applied for the synthesis of the $LiFePO_4$/C composite powder.[13] Commercial quantitative filter paper was used both as a template and a carbon source. Filter paper was soaked in the precursor solution with stoichiometric amounts of Li^+, Fe^{2+} and PO_4^{3-} and introduced for a short period of time to the previously heated furnace at 700 °C, in an

inert atmosphere. As it is consisting of at least 98 wt. % of α-cellulose, filter paper easily degrades to carbon when exposed to a high temperature in an inert atmosphere. The Rietveld refinement confirmed that well-ordered nanocrystallites were obtained. The obtained powder showed an excellent electrochemical performance during galvanostatic cycling. However, the shortcoming of the method is a high carbon yield (40 wt. %), which reduces the energy density of the powder, making its control impossible.

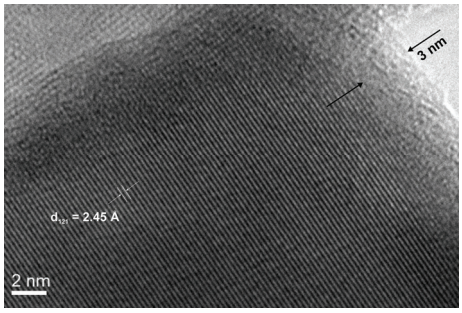

Fig. 3. HRTEM image of the F-doped $LiFePO_4$/C powder. Amorphous carbon film, with a thickness of 3 nm, is deposited on the (121) crystal plane of the orthorhombic $LiFePO_4$.

Other carbon sources that were investigated for the preparation of $LiFePO_4$/ /C composites are various dicarboxylic acids.[14] Freeze drying was employed for the preparation of the precursor powder that was further annealed at 700 °C. It was shown that the amount of the *in situ* formed carbon was not proportional to the carbon content of the used acid. The thermal behaviour of the acids in an inert atmosphere determined the amount of the *in situ* formed carbon.

An one-pot synthesis of pure $LiFePO_4$ particles was conducted by the emulsion-mediated solvothermal route at a low temperature (180 °C).[15] The quaternary emulsions of Triton X-100/cyclohexane/*n*-hexanol/water were solvothermally treated for various time periods, with or without the inclusion of stirring. A drastic dissimilarity in morphology was observed when different modes of solvothermal treatment were applied. During the solvothermal treatment, stirring preserved the formation of micelles, which enabled modified Ostwald ripening during the formation of the polycrystalline material. As a consequence, the anisotropic crystallites with the most exposed {100} facet were grown. This study raises the possibility of tailoring the particle morphology by the emulsion-mediated solvothermal treatment.

Besides $LiFePO_4$, Li_2FeSiO_4 was also investigated as a cathode material for lithium-ion batteries. The solid-state method was employed for the synthesis of composite of monoclinic Li_2FeSiO_4 and carbon.[16] A detailed crystal structure refinement, conducted through a combined X-ray diffraction and Mössbauer spectroscopy study, has revealed that the crystal structure is prone to the so-

-called anti-site defect, where a part of iron ions occupy the lithium tetrahedral positions within a monoclinic $P2_1/n$ crystal symmetry. A bond-valence energy landscape calculation suggested that Li conductivity was two-dimensional in the (101) plane. During galvanostatic cyclings, the structure rearranged into an inverse β_{II} polymorph.

The concept of cellulose matrix templating[13] was further developed for the synthesis of Li_2FeSiO_4/C by the use of water soluble methylcellulose instead of insoluble cellulose.[17] In this way, it was possible to achieve homogeneous mixing of the starting compounds and to control the amount of the *in situ* formed carbon in the composite powder. The percentage of carbon in the composite powder was linearly proportional to the amount of methylcellulose in the precursor. With an increase of carbon content, the mean particle diameter decreased, while electrical conductivity increased, mutually resulting in an improved electrochemical performance.

4. FUNCTIONAL CERAMICS WITH IMPROVED ELECTRICAL AND OPTICAL PROPERTIES

Barium titanate stannate ($BaTi_{1-x}Sn_xO_3$, BTS) materials are very important in the electroceramic industry, since they have a relatively high dielectric permittivity, small dielectric loss and a low leakage current. Along with practical applications in ceramic capacitors, BTS materials are important for the preparation of functionally graded materials (FGMs), since BTS FGMs have a relatively high dielectric permittivity in a wide temperature range.

Although detailed examinations of the dielectric properties of BTS depending on the tin content have been conducted over the years and reported in many papers, the correlation between the structural parameters and the tin content have not been established. For that reason, we chose to study the phase evolution in $BaTi_{1-x}Sn_xO_3$ (x = 0, 0.025, 0.05, 0.07, 0.10, 0.12, 0.15 and 0.20) compounds as a function of Sn for Ti substitution.[18] For a detailed analysis of the crystal structure, the Rietveld refinement of XRD data was performed; according to the results it was established that a gradual increase of the Sn content in $BaTi_{1-x}Sn_xO_3$ caused the transition of the crystal structure from tetragonal (P4mm) for $0 \le x \le 0.07$, *via* coexistence of tetragonal (P4mm) and cubic ($Pm\bar{3}m$) for the powder with x = 0.1, to cubic ($Pm\bar{3}m$) for x = 0.12, 0.15 and 0.20. The phase evolution and the crystal structure of BTS were confirmed by HRTEM and SAED analyses, while Raman spectroscopy suggested a lower local ordering, compared to the average symmetry. Furthermore, the Rietveld analysis of neutron powder diffraction (NPD) data have been used to gain complete insight into the evolution of the BTS crystal structure. The results obtained from NPD data are somewhat different from those determined from XRD data. Actually, the crystal structure of the powder with x = 0 shows the best agreement with a tetragonal (P4mm) space

group; BTS powders with $0.025 \leq x \leq 0.07$ contain a mixture of tetragonal (P4mm) and orthorhombic (Amm2) space groups; in the powders with $x = 0.1$ and 0.12 rhombohedral (R3m) and cubic ($Pm\bar{3}m$) space groups coexist, while those with $x = 0.15$ and 0.20 have undistorted cubic ($Pm\bar{3}m$) space groups. The discrepancy between crystal structures obtained from XRD and NPD data can be explained by the fact that NPD is a more appropriate technique for the characterization of $BaTi_{1-x}Sn_xO_3$, a crystal structure with heavy Ba ions and light oxygen, allowing for a more precise determination of the Ba–O bond distances, fractional atomic coordinates and displacement parameters.[19]

It is known that during the sintering of FGMs, the anisotropic densification occurs and that its extent depends on the heating rate. Therefore, in order to prepare defect-free FGMs, it is very important do develop a sintering strategy. We determined the coefficient of shrinkage anisotropy during the sintering of BTS2.5/BTS15 FGM at heating rates of 2, 5, 10 and 20 °C min^{-1}.[20] BTS2.5/BTS15 FGM has been chosen since it had a large concentration gradient which implied a gradient of the anisotropy coefficient. The concept of the master sintering curve was used to estimate the effective activation energy for the sintering of BTS2.5/ /BTS15 FGMs and it was compared to those for the BTS2.5 and BTS15 graded layers. The values of 359.5 and 340.5 kJ mol^{-1} were obtained for the BTS2.5 and BTS15 graded layers, respectively, whereas for the sintering of the entire BTS2.5/BTS15 FGMs the value of 460 kJ mol^{-1} was obtained. The difference in the effective activation energy of ~100 kJ mol^{-1} can be attributed to a potential insulator interlayer formed between graded layers during uniaxial pressing. The electrical characteristics of BTS2.5/BTS15 FGMs and the influence of the concentration gradient on intrinsic and microstructural features were determined by impedance spectroscopy. The activation energy of BTS2.5/BTS15 FGMs, separately for grain interior and grain boundary, were calculated. It was established that the activation energy deduced from grain-interior conductivity retained the intrinsic properties of BTS materials and was influenced neither by the tin/titanium concentration gradient, nor by the heating rate. Quite oppositely, the activation energy for the grain boundary conductivity was influenced by macrostructural (shrinkage anisotropy) and microstructural development (density and average grain size). These results confirm that by tailoring the heating rate during sintering of FGMs their electrical features can be tailored, too.

We also studied the effects of various sintering approaches on the microstructure and electrical properties of $CaCu_3Ti_4O_{12}$ (CCTO) ceramics[21]. The sinterability of CCTO powders was investigated during the non-isothermal sintering performed by four different heating rates. Based on the non-isothermal sintering behaviour, experiments with conventional (CS) and two-step sintering (TSS) were carried out and it was shown that TSS resulted in microstructural refinement. The electrical properties of sintered ceramics were investigated in the med-

ium-frequency and microwave regions. The measurement results show a high specific resistivity at room temperature, a high relative permittivity at 1 kHz in a wide temperatures interval, as well as high values of dielectric permittivity at resonant frequency. The combination of capacitance behaviour and high dielectric permittivity in the MW range promote the potential use of such materials for the preparation of high dielectric planar antennas, applicable in microelectronics. The XRD measurements of the investigated samples confirmed that difference in electrical characteristics was a consequence of microstructural changes, rather than phase composition, since the only phase present in all samples corresponded to pure CCTO crystal phase. This fact highlights the role of the sintering strategy development in preparing appropriate microstructures with desirable electrical properties.

A series of ZnO powders with the same phase composition and average crystallite size but with different average particle sizes and morphology – from micro-rods to nano-spheres – were prepared by a simple and cost-effective, low--temperature hydrothermal procedure.[22] In order to investigate the effect of the particle size and morphology on the optical properties of ZnO UV–Vis diffuse reflectance spectroscopy (DRS) measurements were performed. The results of the UV–Vis DRS measurements show that: 1) all of the synthesized ZnO powders have enhanced visible light absorption compared to bulk ZnO and 2) that the the modification of particle size and morphology from nano-spheres to micro--rods resulted in an increased absorption. The enhanced visible light absorption of the ZnO powders was caused by two phenomena: 1) the existence of lattice defects (oxygen vacancies and zinc interstitials) and 2) the particle surface sensitization by PVP. Besides, the fact that micro-rods absorbed a larger amount of light than nanosized particles can be explained by a longer optical path for light transport through micro-rods than through submicronic particles or nanoparticles, resulting in a greater absorption capacity.

We studied the influence of poly(ethylene oxide) (PEO) molecular weight on the photocatalytic activity of ZnO/PEO nanostructured composites.[23] Microwave processing was used to prepare ZnO nanoparticles with a high density of intrinsic crystal defects responsible for visible light absorption and enhanced photocatalytic efficiency. To further enhance the photocatalytic activity of ZnO nanoparticles, oxygen interstices were supplied *via* a composite with PEO. To examine the influence of the polymer molecular weight on the photocatalytic activity of the prepared composites, we used PEO with molecular weight of 200,000, 600,000 and 900,000. The effect of PEO molecular weights on the photocatalytic activity of ZnO/PEO composites was examined *via* the de-colorization of methylene blue (MB) under direct sunlight irradiation. A great efficiency of MB decolorization was found and the enhanced photocatalytic activity of ZnO/PEO composites was attributed to: 1) the lattice defects introduced in ZnO crystal

structure by rapid microwave processing and 2) the presence of PEO as a source of oxygen interstitials. To confirm and further clarify the experimental results, we also performed *ab initio* calculations based on the density functional theory (DFT). Our calculations support the assumption that the improved visible light photocatalytic activity can be caused by a band gap narrowing, due to the presence of intrinsic defect states.

5. FULL DENSITY NANOSTRUCTURED CALCIUM PHOSPHATE AND FUNCTIONALLY-GRADED MATERIALS

A segment of our studies was dedicated to the processing of stoichiometric (SHAp) and calcium-deficient hydroxyapatite (CDHAp) nanopowders to develop fully dense nanostructured bioceramics by pressureless sintering. The sintering behaviour of SHAp and CDHAp, prepared by chemical precipitation and hydrothermal processing, was investigated by non–isothermal, classical (CS), and two step sintering (TSS) procedures.[24–26] CS and TSS were applied on CDHAp nano--powder, in order to design dense, fine-grained biphasic calcium phosphate (BCP) ceramics.[24] It was shown that the TSS method had significant advantages compared to the CS method in the processing of BCP ceramics; the TSS experiment resulted in fully dense, uniform, fine-grained BCP ceramics with an average grain size of 375 nm, while the CS yielded micro-meter, non-uniform grains. Another advantage of the TSS approach was a lower sintering temperature, which resulted in the absence of α-tricalcium phosphate (α-TCP) in the two-step sintered sample and which might have beneficial effects on the biological and mechanical response of BCP ceramics. Furthermore, the TSS processed samples showed improved mechanical properties, in terms of both hardness and fracture toughness, compared to the conventionally sintered samples; the fracture toughness of 1.11 MPa·m$^{1/2}$ and the hardness of 4.9 GPa of the TSS-processed samples were in good agreement with those obtained by the application of other, more sophisticated sintering techniques.

Furthermore, we found that the heating rate had a significant influence on the sintering behaviour of CDHAp, where the faster heating resulted in better densification, probably as a consequence of the delayed onset of CDHAp phase transformation into a mixture of HAp and β-TCP.[25] These findings are expected to enable to tailor the final microstructural properties of BCPs, as well as to achieve bioreactivity through an appropriate HAp/β-TCP ratio. With a valid calibration, from a single starting CDHAp system, it is possible to obtain the final BCP ceramics (sintered and/or granulate) with various microstructural properties and/or phase compositions.

By the low-temperature two-step sintering of SHAp nano-powder, fully dense bioceramics with an average grain size of 75 nm (Fig. 4) were developed.[26] The effective activation energy for sintering was estimated to be 412.6 kJ mol^{-1}

using the concept of the master sintering curve. Diffuse-viscous flow controlled by grain boundary diffusion was proposed as the dominant sintering mechanism. HAp nanoparticles with different bulk and grain boundary regions, in terms of an ordered/disordered microstructure, were found to be advantageous for low-temperature sintering.

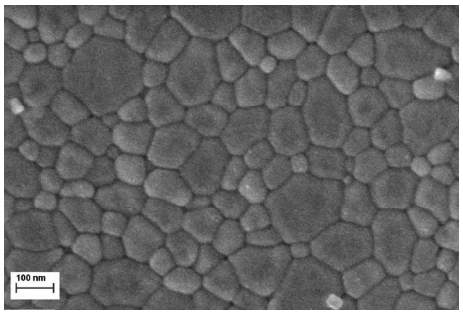

Fig. 4. FE–SEM micrograph of sintered nanostructured HAp.

The influence of grain size refinement, spanning from micrometer *via* submicro-meter to nano-meter scales, on the electrical response of fully dense HAp was studied using impedance spectroscopy. It was found that the nanostructured HAp had enhanced the grain interior conductivity, while the grain boundary contribution to the overall impedance was similar for all microstructures. The activation energy determined for the grain interior conductivity of the nanostructured HAp revealed that OH^- were responsible for conduction, while coarser microstructures probably hosted additional O^{2-} in the crystal lattice, which deteriorated OH^- conduction pathways and the overall conductivity. It was found that conductivity across the grain boundaries was also performed by OH^-, but was independent of grain size. The effects of microstructural refinement on the enhanced electrical properties of hydroxyapatite should be understood from the point of view of the prevented depletion of OH^-, as the main charge carriers, and the shortening of charge transport pathways in dense nano-grained hydroxyapatite ceramics.[27] The chemical precipitation method was also used for the preparation of hydroxyapatite nano-powders in the presence of different concentrations of zirconium ions.[28] HAp/ZrO_2 composites had improved properties, especially mechanical, while biocompatibility was not impaired, when compared to pure HAp. Non-isothermal sintering enables to suppress the reaction between hydroxyapatite and zirconia by limiting it to only calcium phosphates. Stress-induced transformation of tetragonal to monoclinic zirconia was facilitated by a total HAp-to-β-TCP phase transformation.

Nanostructured calcium phosphate functionally graded materials (HAp/BCP FGMs) with simultaneous gradients of density, phase composition, and mechanical properties were fabricated by powder processing and two-step sintering.

The mismatch stress between the adjacent layers, generated during sintering, was successfully reduced by optimizing the phase composition gradient; high-quality FGMs, without excessive shape distortion, delamination, development of cracks and micro-structural failures were obtained. The optimal processing conditions for the preparation of nanostructured ceramics were provided by two-step sintering.[29] The determined spatial change of porosity, phase composition (HAp/β-TCP ratio) and mechanical properties, with a simultaneous enhancement of structural features promoted the fabricated FGMs as functional bioceramics: 1) the average grain size along the overall FGMs was fairly below 100 nm, approximating the dimensions of HAp crystals in natural bone; 2) the amount of β-TCP gradually increased along the FGMs height (the possibility to tailor the HAp/β-TCP ratio in FGMs could ensure an appropriate resorption rate of the artificial bone material); 3) the mechanical properties of the FGMs approximated those of the cortical bone; microhardness was gradually changed from 650 to 115 HV, while Young's modulus graded from 92 to 24 GPa.

6. NANO-CALCIUM PHOSPHATE IN BONE TISSUE ENGINEERING

We synthesized amorphous and crystalline calcium phosphate nano-sized particles, predominantly hydroxyapatite (HAp) in composition, alone and as coated with bioresorptive polymers: poly-lactide-co-glycolide (PLGA) or chitosan (Ch). The properties of the synthesized material in a biological environment were tested on cell lines (*in vitro)* and animals (*in vivo)* in accordance with the standards of ethical committees (Fig. 5).

The ultrasonic processing method was applied to load drugs within HAp/ /PLGA core-shell drug carriers.[30–33] The novel concept involving a simultaneous, controlled release of a drug and a prodrug with different physicochemical properties was applied in order to prolong the release period of antibiotics and estimate their high local concentrations, which are the necessary preconditions for the treatment of some chronic infectious diseases.[30–34] Multifunctional nano-particulate HAp-based powders were prepared for the purpose of: a) either fast or sustained, local delivery of cholecalciferol (D_3) and b) the secondary, osteoconductive and defect-filling effect of the carrier itself.[35] Synthesized nanoparticles (average particle size, d_{50} = 71 nm) of HAp-coated with D_3 loaded PLGA had the zeta potential of –33.4 mV, characteristic for the stable and aggregation-resistant particles. The artificial defects induced in the osteoporotic bone of rats were successfully reconstructed with particles, *in vivo*. The transition of the young bone tissue into mature tissue with the intensive angiogenesis and vascularization was observed when HAp/D_3/PLGA was used as the filler.[35] Newly formed bone tissue was transformed into the mature one using the specific forms, islet-like ossification centres. Original and innovative systems based on PLGA nano-spheres--coated HAp individually[36] or as carriers of various antibiotics and vitamins, justified their further development and the expansion of potential application.

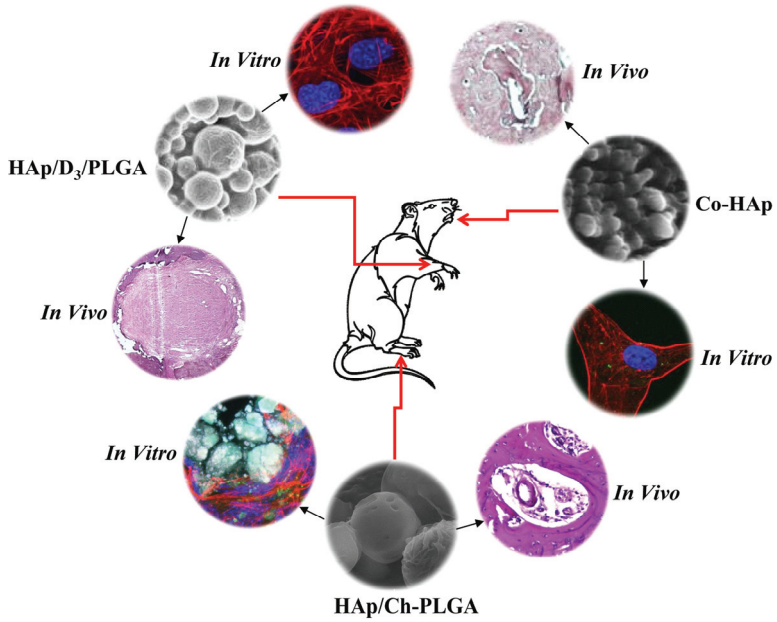

Fig. 5. Biocompatible nanoparticles based on calcium phosphate in bone tissue engineering.

The radioactive ^{125}iodine (^{125}I), a low energy gamma emitter, was used to develop a novel in situ method for the radiolabelling of polymer-coated and uncoated HAp nanoparticles and the investigation of their biodistribution. The labelling method was optimized for ^{125}I-labelling *in situ* during the particle synthesis. The *in vitro* studies in saline and human serum have revealed that ^{125}I remained bound to particles for a period sufficient for further *in vivo* application. Biodistribution and a potential use of ^{125}iodine-labelled particles as organ-targeted carriers were assessed following their intravenous administration. ^{125}I-labeled particles showed completely different behaviour *in vivo* depending on the chemical nature of the carrier: HAp particles mostly targeted the liver, HAp/Ch the spleen and liver and HAp/Ch-PLGA the lungs.[37] Chemotherapeutic derivatives loaded on HAp/Ch-PLGA particles after *in vitro* studies showed a high potential as fine particle platform for a targeted and selective cancer therapy.[38]

Solvent/non-solvent precipitation and freeze-drying were used for the synthesis and processing of HAp coated with Ch or Ch-PLGA nanoparticles with antimicrobial and osteoregenerative properties.[39] A thermogravimetric analysis coupled with on-line mass spectrometry confirmed the coating of the HAp with Ch or Ch-PLGA blend, while *in vitro* and *in vivo* studies justified the concept of blending Ch with PLGA in order to increase the quality of osteogenesis. The quantitative antimicrobial test showed that HAp/Ch-PLGA had some antibacterial properties (*MIC* in mg mL^{-1}): *Pseudomonas aeruginosa* – 6.40, *Staphylo-*

coccus aureus – 6.40 and *Staphylococcus epidermidis* – 3.20). 3-(4,5-Dimethylthiazol-2-yl)-2,5-diphenyltetrazolium bromide (MTT) assay was used to test cytotoxicity and cell viability. By using HAp/Ch-PLGA in the form of a filler, a high level of reparatory ability, with the presence of Haversian canals and cement lines in the reconstructed bone defect, was achieved *in vivo*.[39,40]

Within this phase, the possibility of synthesis and tailoring a new class of HAp in whose crystal lattice Ca^{2+} would be partially substituted with different amounts of Co^{2+} (from 5 to 12 wt. %) was investigated. The Rietveld crystallographic analysis confirmed the substitution of Ca^{2+} with Co^{2+} in the crystal lattice of HAp, during the hydrothermal processing of a precipitate.[41,42] The particles containing 5 and 12 wt. % of Co^{2+} with the average particle size of 63 and 71 nm, respectively, were analysed *in vitro* and *in vivo.* Biological tests revealed the dual nature of nanoparticles Co-HAp, a moderate toxicity during the *in vitro* assay and high inductive ability of bone repair *in* vivo.[41] After the reconstruction of osteoporotic bone tissue (*in vivo*) on more than one hundred animals, it was deduced that the increase in the amount of calcium ions substituted by cobalt, corresponded up to 12 wt. % to an increase in the rate of osteogenesis and to the formation of the new bone tissue with the intensive angiogenesis and vascularisation.

A new sonochemical synthesis approach resulted in the silver nano-particles combined with HAp. When a nitrate precursor was used, the obtained Ag particles were spherical, with up to 20 nm in size.[43] The precursor type (acetates and lactates) had a direct influence on the structure and morphology of the particles: it dictated the formation of hexagonal and cubic Ag phases. During the sonochemical synthesis of nano HAp/Ag composite, HAp had a role of a templating agent. Larger HAp particles adhered to the surface of plate-like HAp, the smaller ones were embedded within these plates, while Ag ions were incorporated within the HAp structure. The needle-like nanoparticles of HAp, obtained by precipitation, served as an adequate carrier of spherical particles of fullerenole ($C_{60}(OH)_x$), known for its antioxidative properties. Using sonochemical processing on the frequency of 20 kHz, HAp particle surface with ζ potential of –2.5 mV was modified with fullerenol particles to ζ potential of –25.0 mV. The spherical particles of $C_{60}(OH)_x$ were homogeneously united using hydrogen bonds with primary needle-like HAp particles into bigger ones, with average sizes of 100 to 350 nm.[44] Thermodynamic phenomena at the interface between HAp particles and bioresorbable polymers during synthesis can be significant for the overall understanding of composite behaviour during *in vitro* and *in vivo* studies. The following thermodynamic functions were studied using inverse gas chromatography: partial molar Gibbs energy, partial molar entalpy of mixing, the sorption molar Gibbs energy, etc. The obtained results established not only a significance of

polymer share in the composite for the surface properties of HAp, but also the selectivity of solutions usable during synthesis and processing.[45]

7. BIODEGRADABLE MICRO- AND NANO-PARTICLES FOR THE CONTROLLED DELIVERY OF MEDICAMENTS

Numerous groups of different micro and nano multifunctional particles and scaffolds based on poly(lactide-co-glycolide) (PLGA)[46–48] or poly(ε-caprolactone) (PCL)[49] as a controlled drug delivery system were synthesized. Silver nano-particles (AgNps) were prepared by the modified chemical reduction with poly (α,γ,L-glutamic acid) (PGA) as a capping agent and encapsulated in the PLGA polymer matrix. Highly stable, uniform and spherical PGA-capped AgNps in the 5–40 nm size range were uniformly distributed in the PLGA matrix.[50] A four-component method was used to synthesize poly(α,γ,L-glutamic acid)-capped silver nanoparticles with nearly spherical, multiply twinned structures, promising for a variety of applications, ranging from catalysis to electronics, surface plasmon resonance, and biomedical research.[51] Poly(α,γ,L-glutamic acid) was used as a capping agent to protect silver nanoparticles from agglomeration as well as to increase their biocompatibility.[52] An emulsifying procedure was used in combination with freeze-drying to prepare multifunctional PLGA spheres encapsulating poly(L-glutamic acid)-capped silver nanoparticles (AgNpPGA, Fig. 6) with ascorbic acid (vitamin C, AscH). We synthesized PLGA/AgNpPGA/AscH spheres with combined osteoinductive, antioxidative and antimicrobial activities.[46] The encapsulation efficiency of AgNpPGA/ascorbic acid within PLGA was determined to be >90 %. The entire amount of encapsulated ascorbic acid was released in two months, whereas the AgNpPGAs completely degraded in three months. The particles did not affect the viability of human hepatoma G2 (HepG2) cells; moreover, they showed an extended antimicrobial activity against gram-positive methicillin-resistant *S. aureus* (MRSA; ATCC 43300), a clinical isolate of MRSA (hospital strain), and *E. faecalis* (ATCC 29212), gram-negative bacteria *E. coli* (ATCC 25922), *K. pneumoniae* (ATCC 13889) and *P. aeruginosa* (ATCC 27853), and *C. albicans* yeast (ATCC 10231). The nanoparticles appeared to be capable of delivering ascorbate to the cells, which was evidenced

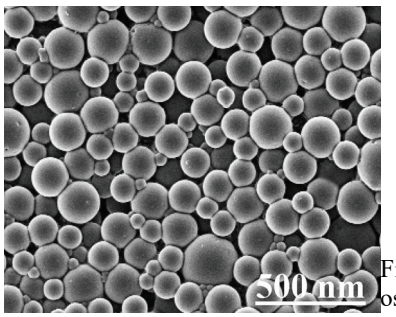

Fig. 6. PLGA/AgNpPGA/AscH particles with combined osteoinductive, antioxidative and antimicrobial activities.

by the significant decrease in the level of superoxides in human umbilical vein endothelial cells and which could have a therapeutic potential in preventing the oxidative stress.[46,53]

The introduction of various porogens and the understanding of their effect on the morphology and pore-formation in PLGA particles were explored with the aim to prevent the delayed drug release in the early phases of degradation and undesired therapeutic side effects associated with it. It was established that the synthesized PLGA nano-spheres were not inducers of intracellular reactive oxygen species (ROS) formation, while sodium chloride was chosen as the optimum porogen.[54] Different types of polyelectrolytes as stabilizers and cryoprotectants were used in the synthesis of nano- and micro-particles of PCL.[49,55] The particles obtained using poly(α,γ,L-glutamic acid) as a stabilizer were spherical, with smooth surfaces.[49] The cryoprotection with 1 % glucose solution was optimal for obtaining uniform, spherical, but also biocompatible PCL nanoparticles for biomedical applications.[55] Smooth and uniform PCL nanospheres with sizes below 200 nm showed no cytotoxicity, a low potential for ROS[56] generation and a low genotoxicity potential during *in vitro* test.[57]

8. CONCLUSIONS

The control of the morphological and physicochemical properties of nano-particles and functional materials based on them is of primary significance for the further development of nanotechnologies. By implementing the MODENAFUNA project III45004, the researchers showed possible ways and methods for designing a wide range of nanoparticulate and nanocrystalline materials of broader significance. The achieved project results include a wide range of outputs, as presented in Supplementary material to this paper.

SUPPLEMENTARY MATERIAL

General evaluation of the project results are available electronically at the pages of journal website: http://www.shd.org.rs/JSCS/, or from the corresponding author on request.

Acknowledgements. The research presented in this paper was supported by the Ministry of Education, Science and Technological Development of the Republic of Serbia, under Project No. III45004, “Molecular designing of nanoparticles with controlled morphological and physicochemical characteristics and functional materials based on them”. The idea to write this paper arose from a discussion with FEMS (The Federation of European Materials Societies) officers while working on MATCH (MATerials Common House) project. The authors would like to thank Dr. Slobodan Milonjić for reading text.

ИЗВОД

МОЛЕКУЛАРНО ДИЗАЈНИРАЊЕ НАНОЧЕСТИЦА И ФУНКЦИОНАЛНИХ МАТЕРИЈАЛА

НЕНАД Л. ИГЊАТОВИЋ, СМИЉА МАРКОВИЋ, ДРАГАНА ЈУГОВИЋ и ДРАГАН П. УСКОКОВИЋ

Институт техничких наука Српске академије наука и уметности, Кнез Михајлова 35/4, 11000 Београд

Интердисциплинарни истраживачки тим реализовао је програм под називом "Молекуларно дизајнирање наночестица са контролисаним морфолошким и физичко–хемијских својствима и функционалних материјала на њиховој бази (МОДЕНАФУНА)", у периоду 2011–2016. година, и при том стекао низ нових знања, а у циљу унапређења наноматеријала и нанотехнологија. Програм је обухватио шест међусобно повезаних целина дизајнирања и контроле морфолошких и физичко–хемијских својстава наночестица и функционалних материјала користећи иновативне методе синтезе и процесирања: 1) неорганске наночестице, 2) катодни материјали за литијум-јонске батерије, 3) функционална керамика са побољшаним електричним и оптичким својствима, 4) високо-густи нано-структурни калцијум-фосфат и функционално градијентни материјали, 5) нано-калцијум-фосфатне честице у инжењерству коштаног ткива и 6) биоразградиве микро- и наночестице за контролисану расподелу лекова.

(Примљено 7. децембра, ревидирано 15. децембра, прихваћено 23. децембра 2016)

REFERENCES

1. V. Uskoković, C. Hoover, M. Vukomanović, D. P. Uskoković, T. A. Desai, *Mater. Sci. Eng., C* **33** (2013) 3362
2. Z. S. Stojanović, N. Ignjatović, V. Wu, V. Žunič, L. Veselinović, S. Škapin, M. Miljković, V. Uskoković, D. Uskoković, *Mater. Sci. Eng., C* **68** (2016) 746
3. Ž. Janićijević, M. J. Lukić, L. Veselinović, *Mater. Des.* **109** (2016) 511
4. S. Marković, L. Veselinović, M. J. Lukić, L. Karanović, I. Bračko, N. Ignjatović, D. Uskoković, *Biomed. Mater.* **6** (2011) 45005
5. V. Uskoković, D. P. Uskoković, *J. Biomed. Mater. Res., B: Appl. Biomater.* **96** (2011) 152
6. Z. Stojanović, M. Otoničar, J. Lee, M. M. Stevanović, M. P. Hwang, K. H. Lee, J. Choi, D. Uskoković, *Colloids Surfaces, B: Biointerfaces* **109** (2013) 236
7. J. Choi, S. Park, Z. Stojanović, H. S. Han, J. Lee, H. K. Seok, D. Uskoković, K. H. Lee, *Langmuir* **29** (2013) 15698
8. A. Stanković, L. Veselinović, S. D. Škapin, S. Marković, D. Uskoković, *J. Mater. Sci.* **46** (2011) 3716
9. A. Stanković, S. Dimitrijević, D. Uskoković, *Colloids Surfaces, B: Biointerfaces* **102** (2013) 21
10. D. Jugović, M. Mitrić, M. Kuzmanović, N. Cvjetićanin, S. Škapin, B. Cekić, V. Ivanovski, D. Uskoković, *J. Power Sources* **196** (2011) 4613
11. M. Milović, D. Jugović, N. Cvjetićanin, D. Uskoković, A. S. Milošević, Z. S. Popović, F. R. Vukajlović, *J. Power Sources* **241** (2013) 70
12. D. Jugović, M. Mitrić, M. Milović, N. Cvjetićanin, B. Jokić, A. Umićević, D. Uskoković, *Ceram. Int.* **43** (2017) 3224
13. D. Jugović, M. Mitrić, M. Milović, B. Jokić, M. Vukomanović, D. Suvorov, D. Uskoković, *Powder Technol.* **246** (2013) 539

14. M. Kuzmanović, D. Jugović, M. Mitrić, B. Jokić, N. Cvjetićanin, D. Uskoković, *Ceram. Int.* **41** (2015) 6753
15. D. Jugović, M. Mitrić, M. Kuzmanović, N. Cvjetićanin, S. Marković, S. Škapin, D. Uskoković, *Powder Technol.* **219** (2012) 128
16. D. Jugović, M. Milović, V. N. Ivanovski, M. Avdeev, R. Dominko, B. Jokić, D. Uskoković, *J. Power Sources* **265** (2014) 75
17. M. Milović, D. Jugović, M. Mitrić, R. Dominko, I. Stojković-Simatović, B. Jokić, D. Uskoković, *Cellulose* **23** (2016) 239
18. L. Veselinović, M. Mitrić, L. Mančić, M. Vukomanović, B. Hadžić, S. Marković, D. Uskoković, *J. Appl. Crystallogr.* **47** (2014) 999
19. L. Veselinović, M. Mitrić, M. Avdeev, S. Marković, D. Uskoković, *J. Appl. Crystallogr.* **49** (2016) 1726
20. S. Marković, D. Uskoković, in *Advances in Electroceramic Materials II*, K. M. Nair, Shashank Priya, Eds., Wiley, Hoboken, NJ, 2010, p. 97
21. S. Marković, M. Lukić, Č. Jovalekić, S. D. Škapin, D. Suvorov, D. Uskoković, in *Processing and Properties of Advanced Ceramics and Composites V: Ceramic Transactions, Vol. 240*, N. P. Bansal, J. P. Singh, S. Ko, R. H. R. Castro, G. Pickrell, N. J. Manjooran, M. Nair, G. Singh, Eds, Wiley, Hoboken, NJ, 2013, p. 337
22. A. Stanković, Z. Stojanović, L. Veselinović, S. D. Škapin, I. Bračko, S. Marković, D. Uskoković, *Mater. Sci. Eng., B: Solid-State Mater. Adv. Technol.* **177** (2012) 1038
23. S. Marković, V. Rajić, A. Stanković, L. Veselinović, J. Belošević-Čavor, K. Batalović, N. Abazović, S. D. Škapin, D. Uskoković, *Sol. Energy* **127** (2016) 124
24. M. Lukić, Z. Stojanović, S. D. Škapin, M. Maček-Kržmanc, M. Mitrić, S. Marković, D. Uskoković, *J. Eur. Ceram. Soc.* **31** (2011) 19
25. M. J. Lukić, L. Veselinović, Z. Stojanović, M. Maček-Kržmanc, I. Bračko, S. D. Škapin, S. Marković, D. Uskoković, *Mater. Lett.* **68** (2012) 331
26. M. J. Lukić, S. D. Škapin, S. Marković, D. Uskoković, *J. Am. Ceram. Soc.* **95** (2012) 3394
27. M. J. Lukić, Č. Jovalekić, S. Marković, D. Uskoković, *Mater. Res. Bull.* **61** (2015) 534
28. M. J. Lukić, L. Veselinović, M. Stevanović, J. Nunić, G. Dražič, S. Marković, D. Uskoković, *Mater. Lett.* **122** (2014) 296
29. S. Marković, M. J. Lukić, S. D. Škapin, B. Stojanović, D. Uskoković, *Ceram. Int.* **41** (2015) 2654
30. M. Vukomanović, S. D. Škapin, B. Jančar, T. Maksin, N. Ignjatović, V. Uskoković, D. Uskoković, *Colloids Surfaces, B: Biointerfaces* **82** (2011) 404
31. M. Vukomanović, S. D. Škapin, I. Poljanšek, E. Žagar, B. Kralj, N. Ignjatović, D. Uskoković, *Colloids Surfaces, B: Biointerfaces* **82** (2011) 414
32. M. Vukomanović, T. Zavašnik-Bergant, I. Bračko, S. D. Škapin, N. Ignjatović, V. Radmilović, D. Uskoković, *Colloids Surfaces, B: Biointerfaces* **87** (2011) 226
33. M. Vukomanović, I. Šarčev, B. Petronijević, S. D. Škapin, N. Ignjatović, D. Uskoković, *Colloids Surfaces, B: Biointerfaces* **91** (2012) 144
34. N. L. Ignjatović, P. Ninkov, R. Sabetrasekh, S. P. Lyngstadaas, D. P. Uskoković, *Biomed. Mater. Eng.* **24** (2014) 1647
35. N. Ignjatović, V. Uskoković, Z. Ajduković, D. Uskoković, *Mater. Sci. Eng., C* **33** (2013) 943
36. M. Đ. Vukelić, Ž. J. Mitić, M. S. Miljkovic, J. M. Živković, N. L. Ignjatović, D. P. Uskoković, J. Ž. Živanov-Čurlis, P. J. Vasiljevic, S. J. Najman, *J. Appl. Biomater. Funct. Mater.* **10** (2012) 43

37. N. Ignjatović, S. Vranješ Djurić, Ž. Mitić, D. Janković, D. Uskoković, *Mater. Sci. Eng., C* **43** (2014) 439
38. N. L. Ignjatović, K. M. Penov-Gaši, V. M. Wu, J. J. Ajduković, V. V Kojić, D. Vasiljević-Radović, M. Kuzmanović, V. Uskoković, D. P. Uskoković, *Colloids Surfaces, B: Biointerfaces* **148** (2016) 629
39. N. Ignjatović, V. Wu, Z. Ajduković, T. Mihajilov-Krstev, V. Uskoković, D. Uskoković, *Mater. Sci. Eng., C* **60** (2016) 357
40. Z. R. Ajduković, T. M. Mihajilov-Krstev, N. L. Ignjatović, Z. Stojanović, S. B. Mladenović-Antić, B. D. Kocić, S. Najman, N. D. Petrović, D. P. Uskoković, *J. Nanosci. Nanotechnol.* **15** (2015) 1
41. N. Ignjatović, Z. Ajduković, V. Savić, S. Najman, D. Mihailović, P. Vasiljević, Z. Stojanović, V. Uskoković, D. Uskoković, *J. Mater. Sci. Mater. Med.* **24** (2013) 343
42. N. Ignjatović, Z. Ajduković, J. Rajković, S. Najman, D. Mihailović, D. Uskoković, *J. Bionic Eng.* **12** (2015) 604
43. M. Vukomanović, I. Bračko, I. Poljanšek, D. Uskoković, S. D. Škapin, D. Suvorov, *Cryst. Growth Des.* **11** (2011) 3802
44. A. Djordjević, N. Ignjatović, M. Seke, D. Jović, D. Uskoković, Z. Rakočević, *J. Nanosci. Nanotechnol.* **15** (2015) 1538.
45. A. B. Nastasović, N. L. Ignjatović, D. P. Uskoković, D. D. Marković, B. M. Ekmeščić, D. D. Maksin, A. E. Onjia, *J. Mater. Sci.* **49** (2014) 5076.
46. M. Stevanović, V. Uskoković, M. Filipović, S. D. Škapin, D. Uskoković, *ACS Appl. Mater. Interfaces* **5** (2013) 9034–9042
47. S. R. Vučen, G. Vuleta, A. M. Crean, A. C. Moore, N. Ignjatović, D. Uskoković, *J. Pharm. Pharmacol.* **65** (2013) 1451
48. M. Stevanović, N. Filipović, J. Djurdjević, M. Lukić, M. Milenković, A. Boccaccini, *Colloids Surfaces, B: Biointerfaces* **132** (2015) 208
49. N. Filipovic, M. Stevanovic, A. Radulovic, V. Pavlovic, D. Uskokovic, *Compos., B:Engineering* **45** (2013) 1471
50. M. M. Stevanović, S. D. Škapin, I. Bračko, M. Milenković, J. Petković, M. Filipič, D. P. Uskoković, *Polymer (Guildf.)* **53** (2012) 2818
51. M. Stevanović, I. Savanović, V. Uskoković, S. Škapin, I. Bračko, U. Jovanović, D. Uskoković, *Colloid Polym. Sci.* **290** (2012) 221
52. M. Stevanović, B. Kovačević, J. Petković, M. Filipič, D. Uskoković, *Int. J. Nanomedicine* **6** (2011) 2837
53. M. Stevanović, I. Bračko, M. Milenković, N. Filipović, J. Nunić, M. Filipič, D. P. Uskoković, *Acta Biomater.* **10** (2014) 151
54. M. Stevanović, V. Pavlović, J. Petković, M. Filipič, D. Uskoković, *Express Polym. Lett.* **5** (2011) 996
55. P. Stupar, V. Pavlović, J. Nunić, S. Cundrič, M. Filipič, M. Stevanović, *J. Drug Deliv. Sci. Technol.* **24** (2014) 191
56. J. Petković, B. Žegura, M. Stevanović, N. Drnovšek, D. Uskoković, S. Novak, M. Filipič, *Nanotoxicology* **5** (2011) 341
57. N. Filipović, M. Stevanović, J. Nunić, S. Cundrič, M. Filipič, D. Uskoković, *Colloids Surfaces, B: Biointerfaces* **117** (2014) 414.